Journal of Magnetics 16(3), 246-252 (2011) http://dx.doi.org/10.4283/JMAG.2011.16.3.246

Full Wave Cockroft Walton Application for Transcranial Magnetic Stimulation

Sun-Seob Choi[1] and Whi-Young Kim[2]*

[1]*Department of Radiology/Neuro radiology Section, Dong-A University Medical Center, Busan 602-715, Korea*
[2]*Department of Biomedical Engineering, Dong-ju College University, Busan 602-715, Korea*

(Received 1 August 2011, Received in final form 14 September 2011, Accepted 15 September 2011)

A high-voltage power supply has been built for activation of the brain via stimulation using a Full Wave Cockroft-Walton Circuit (FWCW). A resonant half-bridge inverter was applied (with half plus/half minus DC voltage) through a bidirectional power transistor to a magnetic stimulation device with the capability of producing a variety of pulse forms. The energy obtained from the previous stage runs the transformer and FW-CW, and the current pulse coming from the pulse-forming circuit is transmitted to a stimulation coil device. In addition, the residual energy in each circuit will again generate stimulation pulses through the transformer. In particular, the bidirectional device modifies the control mode of the stimulation coil to which the current that exceeds the rated current is applied, consequently controlling the output voltage as a constant current mode. Since a serial resonant half-bridge has less switching loss and is able to reduce parasitic capacitance, a device, which can simultaneously change the charging voltage of the energy-storage condenser and the pulse repetition rate, could be implemented. Image processing of the brain activity was implemented using a graphical user interface (GUI) through a data mining technique (data mining) after measuring the vital signs separated from the frequencies of EEG and ECG spectra obtained from the pulse stimulation using a 90S8535 chip (AMTEL Corporation).

Keywords : full wave, Cockroft-Walton, pulse-forming circuit, serial resonant, half-bridge, stimulation

1. Introduction

In a magnetic stimulation device, electromagnetic force is induced by changes of the current in the magnetic circuit; if the current flowing in the circuit changes, the number of flux linkage per unit current also changes [1-3]. Electromagnetic force is generated in the direction that interrupts such changes, and the relationship of organic electromagnetic force to changes of the current in the magnetic field circuit resulting from the flux linkage per unit current is established by Faraday, Neumann, and Lenz's laws and by magnetic field induction [4-7].

Generating an electric field using an eddy current is the basic principle of the magnetic stimulation device, and this is achieved by delivering strong current pulses to the stimulation coil by generation of a time-varying magnetic field that can sufficiently stimulate the neuromuscular system of the human body [8-11]. The strength of an electric field that generates a time-varying magnetic field is proportional to the changes of the magnetic field throughout time, and it may generate strong pulse changes depending on its duration [12].

The voltage of the main circuit and the peak value of current significantly change between running the coil and discharging the magnetic field in the stimulation coil of the magnetic stimulation device, and a drive circuit, to which the drive of the stimulation coil and the discharge of the magnetic field is directed, is required [13, 14]. The operating frequency of the stimulation coil must be determined by evaluating the efficiency of energy flowing to the coil, and the coupling efficiency may vary with operating frequency.

For multipurpose treatments, the capacity of the stimulation coil must be greater because the stimulating frequency is altered. To enable the stimulation, the stimulating coil generating a magnetic field by discharging a high voltage (several KV) should be equipped with a capacitor that stores the required energy [3]. The capacitor generates a current of several kA by discharging to the stimulating coil, repeating charging and discharging phases within as few as several hundred seconds. To implement

*Corresponding author: Tel: +82-51-200-3449
Fax: +82-51-200-3235, e-mail: ndyag@dongju.ac.kr

stimulation by triggering eddy currents inside human body using a magnetic field in the form of pulse, a power supply is required that has high performance, high-pressure resistance, high repetition, high-speed switching device, and various control techniques [6]. In this study, we suggested a compact magnetic stimulation device, which has several advantages: it generates high voltage with low impact on other devices through a Full Wave Cockroft-Walton Circuit, operates with half of the existing plus/minus DC voltage through a serial resonant half-bridge, and contains a bidirectional switching device.

Such an approach may have several advantages:

1) It is superior in size, weight, and response speed. 2) Since the current-resonant half bridge is the zero current switching (ZCC) type, it has lower switching loss and higher efficiency. 3) Since the circuit configuration is designed for round operation, all residual energy can be utilized. 4) When using a bidirectional switching device, the half bridge can be run half DC voltage used in previous time. 5) Using an AVR Chips (AMTEL corporation), it is four times faster than a programmable integrated controller (AVR), ten times faster than a 8051, supports C language, and has an in system program (ISP) function that allows the program to be changed or modified several times. Moreover, the magnetic stimulation device is controllable by applying a precise operating frequency to the switching device, and the image processed in the graphical user interface (GUI) allows easy monitoring of the brain activity status after measurement.

2. Design

Since the control of current pulse and reliability of the magnetic stimulation device are excellent, output and electrical pulses of high quality can be obtained; therefore, it is suitable for microscopic diagnosis, and it should be used for both diagnosis and treatment of the brain and muscle [7]. To overcome these problems, the correct power density and a variety of controls are important. Methods for controlling operating time and changing the repetition rate of the pulse by converting the output of the stimulation device into pulses can be applied to the density control. To achieve these goals, we suggested a novel approach that generates precise control and radio wave high voltage by controlling a half value of DC voltage and constant control of pulse width using a bidirectional device, ZCS resonant inverter, FW-CW, and Pulse Forming Network (PFN) (the system becomes a PFN).

Fig. 1 displays a new configuration of the magnetic stimulation device composed of a bidirectional device, transformer, zero crossing switching (ZCS), resonant inverter, FW-CW circuit, and PFN circuit. In addition, multiple injections of energy rather than a single high-energy pulse have better permeability and a lower system load. Particularly, the bidirectional device (IGBT: insulated gate bipolar transistor) is composed of a diode for rectification and a switching device, and it is connected to the neutral tab of the DC power supply; therefore, half of the DC power can be applied to the output voltage. The

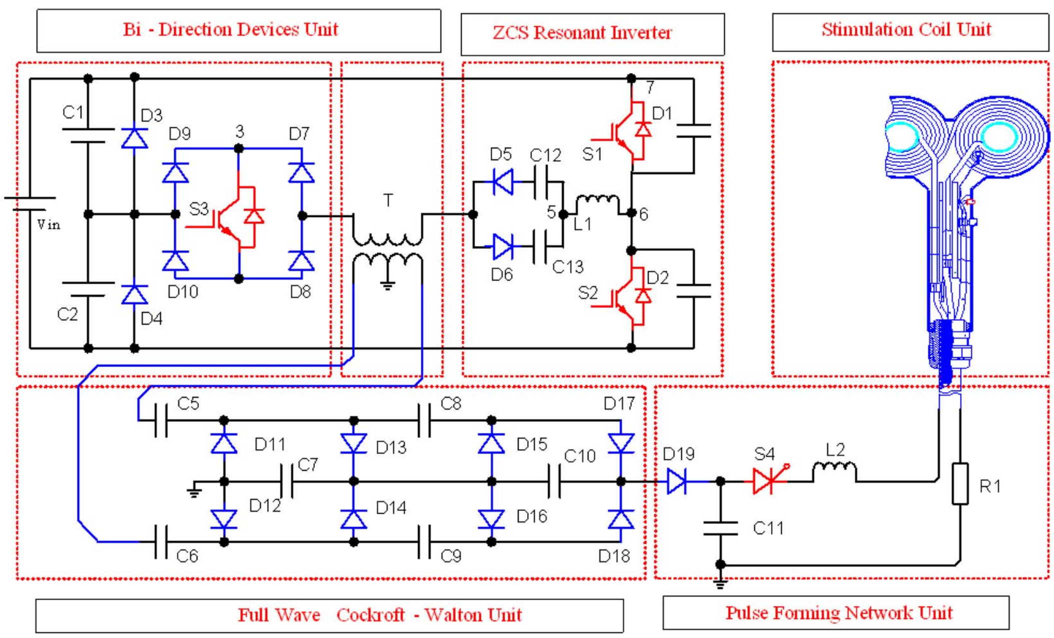

Fig. 1. (Color online) Diagram of the proposed magnetic stimulation device.

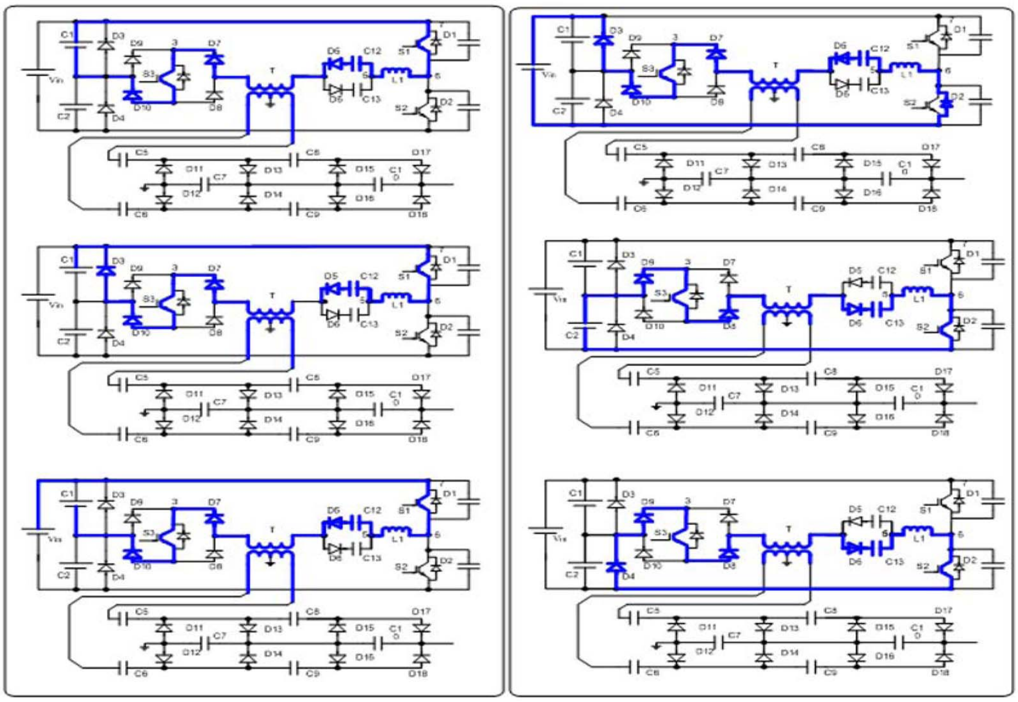

Fig. 2. (Color online) Operation mode of the circuit system.

transformer primarily delivers the control pulse generated by a serial resonant inverter as energy through the FW-CW, and it secondarily delivers energy to the stimulation coil through the RW-CW circuit via the bidirectional device [8]. To configure a pulse forming circuit, a resonant converter was applied to the magnetic stimulation device and was configured to minimize the loss caused by tailing current when powering off through the IGBT, which accommodates high frequencies and reduces switching loss and noise. Since powering the switching device on and off of in zero current is done by modulating the flowing current (inside the switching device and capacitor) as a sine wave, there is – in principle – no switching loss, and it is very efficient at high repetition rates. The operation mode can be classified into the first and second loop modes; the operating sequence is as follows: Fig. 2 indicates the operating mode, and its detailed description is shown below. C1 is charged by the input voltage Vin in the first loop; 0 voltage is applied to C2; and S1 and S2 are in the state where no current is flowing into the stimulation coil. Once S1 is on, the resonant current, which flows through the loop C1-S1-L1-C12-D5-T (FW-CW)-D7-S3-D10-C1 and the loop Vin-S1-L1-C12-D5-T(FW-CW)-D7-S3-D10-D3, supplies energy to T (FW-CW). In addition, after C1 is discharged at time t1, the current flowing in the resonant inductor, L1, flows to the loop L1-C12-D5-T (FW-CW)-D7-S3-D10-L1 and allows Vc1 (the voltage of the resonant capacitor C1) to be zero and clamps Vc2 (the voltage of the resonant capacitor C2) to Vin.

It would be ideal if S1 were off after the resonant current becomes 0; however, due to the nature of coil 1, the tailing current flows continuously. Therefore, if a forced power-off is performed after the calculated power-on time, the resonant current at that time will decrease to 0 as it flows to L1-C12-D5-T (FW-CW)-D7-S3-D10-D3-Vin- L1. At this time, the current is not flowing to C12 because it is blocked by D5, and energy is only supplied to C13. If S2 is turned on after a given period of time, the resonant current will flow to the loop C2-D9-S3-D8-T (FW-CW)-D6-C13-L1-S2-C2 and the loop Vin-C2-D9-S3-D8-T (FW-CW)-D6-C13-S2-Vin, and energy will be supplied to T (FW-CW) by channeling the resonant current to L1 in the direction opposite the initial direction. Moreover, once C2 is discharged, the resonant current of L1 will release energy to T (FW-CW), flowing to the loop L1-S2-D4-D9-S3-D8-T (FW-CW)-D6-C13-L1, and the current will be 0. Vc1 (the voltage of both ends) of C1 (the resonant capacitor) is clamped due to D3, and the operation will repeat.

The two-stage, FW-CW voltage multiplier plays a role in delivering the discharge of the capacitor obtained from high voltage generation to the stimulation coil device. C5 of Fig. 1 displays the transmission of such energy to C10, etc. through a boosting transformer. A FW-CW radio wave is a voltage multiplier, and it converts AC or lower voltage levels to high DC voltage or to a pulsing DC current. The circuit has to be configured in the form of a magnify able ladder to generate high voltage. A voltage multiplier using a capacitor and diode is lighter, cheaper, and much more efficient than a transformer-type multiplier operating for the same amount of time because it is simple to turn a relatively lower voltage to high voltage. The value converted via wave rectification is three times greater than the input voltage. This approach enables the construction of a relatively inexpensive circuit, and it has advantages in processing problems, such as insulation between device components. Among these advantages, the output tab of multiple stages can be created from the multi-tab transformer; and the stimulation coil can be processed as a resistance load while it is discharging. Therefore, the average output voltage value is smaller than 3nVp due to the voltage drop, which is a function of load current. Since the DC current is greater than 3 kV under the quiescent conditions of the cascade rectifier, a circuit of 2 stages is produced, and the boosting pulse transformer has an input voltage value of 230 V due to the peak voltage value, 500 V.

2Nf and a diode, RVT1500 (a fast recovery diode), were used as the capacitors of C5-C18 in the FWCW circuit. Ballast resistance R1 is located between the electrodes of the FWCW circuit and the stimulation coil. These features can restrict the dramatically increasing peak value of discharging current. The increasing frequency is able to decrease voltage and to reduce ripples by running multiplier stacks on the loaded switching power supply. A radio wave voltage doubler is used for the purpose of reducing ripples. This effectively cuts off voltage drops and ripples by doubling the number of charging cycles per second. Input is continuously supplied through the middle tab of the AC transformer. The output voltage of the two-stage FW-CW is shown in Equation (1),

$$V_{out} = 2n^{Vpk} - V_{drop} \tag{1}$$

For example, the circuit voltage opened in the two-stage FW-CW is

$$V_{out} = 2 \times 2 \times V^{pk} \tag{2}$$

and the calculations for adjusting the FW-CW and ripples are shown in the following equation.

$$V_{drop} = \left[\frac{I_{load}}{4Fc}\right]^{*(n^2+2n)} \tag{3}$$

Here, I_{LOAD} is the load current,
C is capacitance stage,
F is AC frequency (Hz), and
N is the number of stages

The following equation can be derived by subtracting V_{drop} from the previous equation.

$$V_{output} = 2n^{vpk} - \left[\frac{I_{load}}{4Fc}\right]^{*(n^2+2n)} \tag{4}$$

The ripple voltage can be calculated using Equation (5), if the capacitor is the same in every stage.

$$V_{ripple} = \left[\frac{I_{load}}{4Fc}\right]^{*(n)} \tag{5}$$

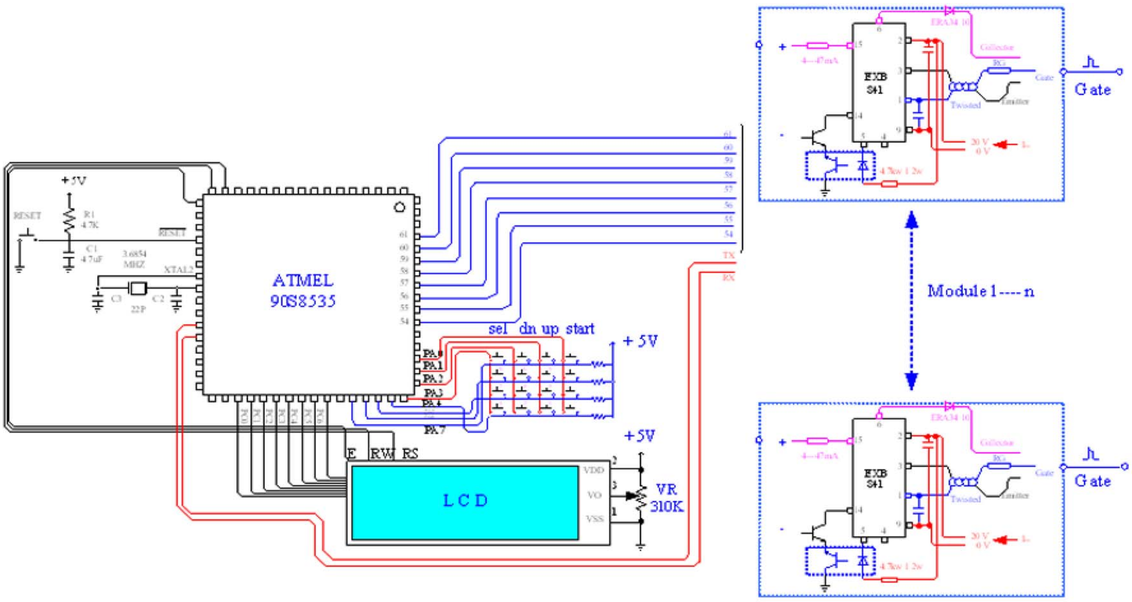

Fig. 3. (Color online) AVR-one-chip control and drive circuit.

The optimal number of stages can be determined using Equation (6) and the given input and output values.

$$N_{optimal} = \mathrm{int}\left[\frac{0.521\,V_{OUT}}{V_{pk}}\right] \qquad (6)$$

Figure 3 indicates the control of the driving pulse for running S1, S2, S3, and the display using an AT90S8535 (AMTEL). The AVR (ATMEL90S8535) supplies delayed, nested, and other pulse types to the drive module (FUJI EXB841) through a keypad. Various types of information can be inputted whenever necessary using the keypad. If the current of the inductor is higher than the preset value or the rating current, it will switch to the constant current control mode, and although there is slight distortion in the output voltage, it will maintain a stable output voltage once the load decreases to a value lower than the constant current. The size of the magnetic field induction of the magnetic stimulation device obtained from the experiment was 0.1-3.1 Tesla, the pulse duration was 250-350 μs, and the stimulation frequency was 0.1-70 Hz.

3. Experimental Results

A wide variation in the voltage rise time patterns of the stimulation coil device depends on the load conditions, when not controlled by the serial resonant inverter. In a non-resonant inverter, the vibration will largely depend on the winding capacity between the leakage inductance of the high-voltage transformer and winding wire caused by switching operation on and off for each inverter cycle. Fig. 4 indicates the output control signal from the AVR in the experiment. Waveform 1 is the timing signal output from AVR ②, and waveforms 2, 3, and 4 are the control output signals from AVRs ①, respectively. Since the S3 signal is generated at a time interval of approximately 16.67 ms, it can be determined that the magnetic stimulation system is running at 60 pps (pulse per second). Fig. 5 shows the output current waveform of the inverter flowing through L1, the operation signals of the half-bridge IGBT, and the operation signals of SCR. Waveform 1 is the output current waveform from the inverter, waveforms 2 and 3 are the operation signals of IGBT S_1 and S_2, respectively, and waveform 4 is the operation signal of SCR S3.

The peak inverter output current initially increases slightly, but it becomes stable as it is being charged. In addition, the peak inverter current flowing through the wheeling diodes connected in parallel with the IGBT gradually decreases. This is due to the gradual charging of C3. Fig. 6 illustrates the experiment patterns of voltage and current on the collector-emitter of the IGBT S1; these patterns also are observed for the bypassed current through the free-wheeling diode D1 when the IGBT S1 is turned off. Waveform 1 (Fig. 7) is the inverter output current waveform at the beginning of the half-bridge switching; waveforms 2 and 3 are the magnified operating signals of IGBT S_1 and S_2, respectively. The operating signals, S_1 and S_2, are set to be turned on/off sequentially according to current resonant time, and the inverter output current

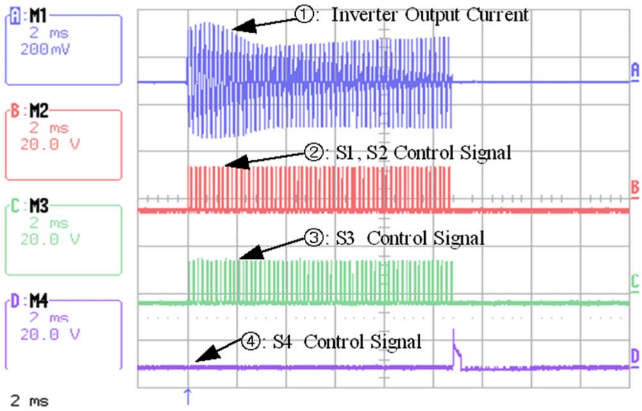

Fig. 5. (Color online) Inverter output current and control signals S1, S2, S3, and S4.

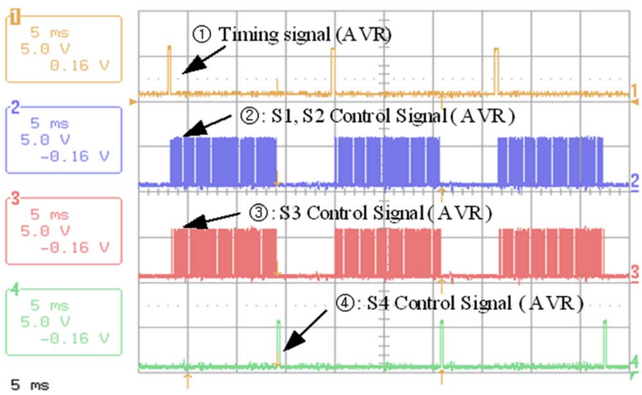

Fig. 4. (Color online) Various signals outputed to the AVR.

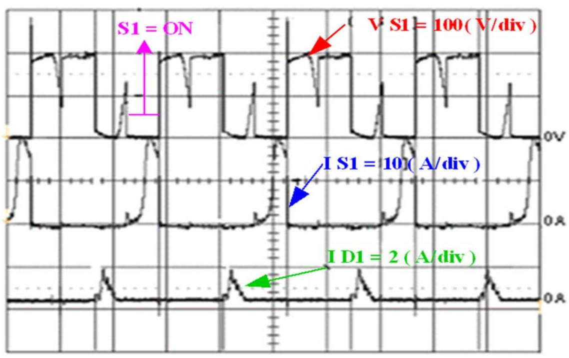

Fig. 6. (Color online) Voltage and current waveforms between the IGBT collector and emitter.

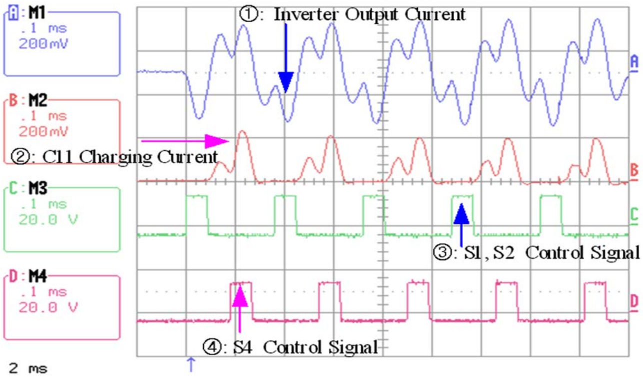

Fig. 7. (Color online) Half-bridge inverter output, charging current, and waveform of the charging current.

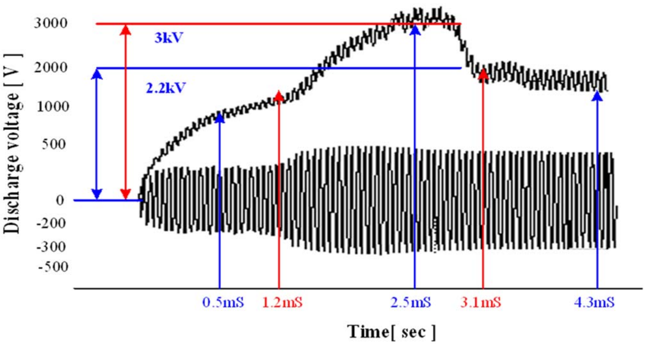

Fig. 8. (Color online) Transient start-up process of the FW-CW.

resonates. Fig. 8 shows the progress of input voltage 230 VDC at an operating frequency of 4.3 kHz when starting operation. In this experiment, the arc discharge striking voltage was set at 3kVDC. In the figure, the arc striking voltage requires 2.45 ms or 19.6 cycles to maneuver the DC-DC converter. Fig. 9 displays the waveforms of the

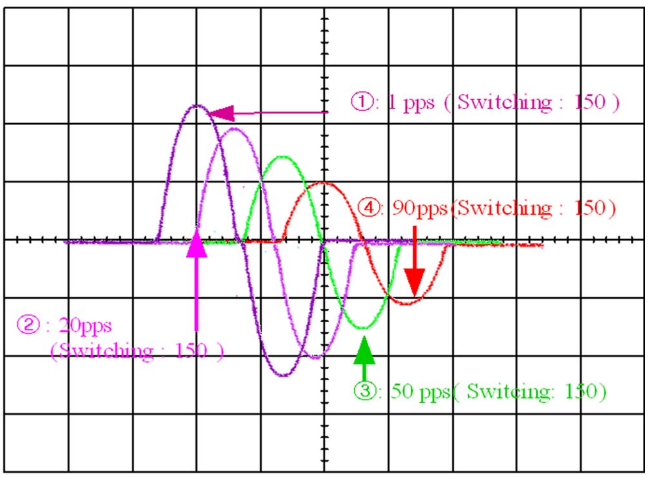

Fig. 9. (Color online) Stimulation current waveforms as a function of changes in repetition rate.

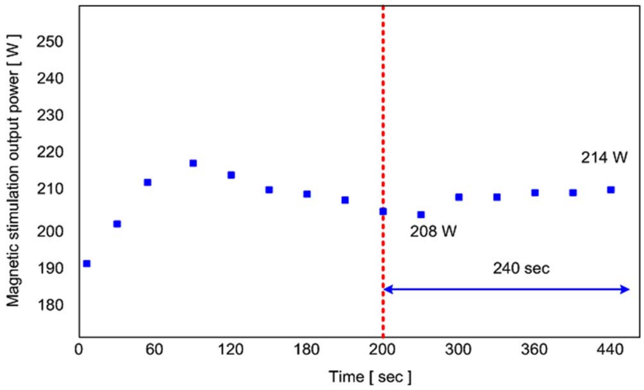

Fig. 10. (Color online) Magnetic Stimulation output power as a time.

stimulation coil current according to the repetition rate when the switching frequency of the half-bridge inverter is 150 Hz. The signals-①, ②, ③, and ④-are the waveforms of the stimulation coil currents at 1, 20, 50, and 90 pps, respectively.

The more the pulse repetition rate increases, the more the peak value of the current decreases slightly; therefore, the higher pulse repetition rate decreases the efficiency in each pulse of the magnetic stimulation device. Therefore, the slope of the output curve of the magnetic stimulation device as a function of the increase of the pulse repetition rate is likely to decrease gradually. Fig. 10 shows Magnetic Stimulation output power as a time. Energy increase due to the high charging voltage in response to the switching frequency increase indicates a peak current increase. As a result, the output energy of the magnetic stimulation device from one pulse will be increased, too. Since the condenser capacity and the value of inductor L3 are kept constant while changing the charging voltage, it can be seen that the FWHM of the current pulse remains constant for approximately 120 μS.

The stimulation pulse of the FWCW-MS is 250 μS, and the stimulation frequency is 10 Hz.

A GUI was developed, and a component software development technology based on the object-oriented technology in the user interface using OLE automation objects was applied to the GUI. Accessibility was enhanced by adapting the ADO technology to which the remote database connection was applied, enabling user programs to be plugged in using components as object controls.

4. Conclusion

In this study, a power supply, which is compact because it did not incorporate a boosting transformer, was used as a magnetic stimulation device. The device can charge the energy storage condenser with rectified DC power at a range of variation from 0 to 820 V using the current resonant half-bridge inverter and Cockcroft-Walton circuit while adjusting the switching frequency and pulse repetition rate (pps) at the same time. It was possible to linearly vary the charging condenser, voltage, and energy and the output energy of the magnetic stimulation device over a single pulse by adjusting the switching frequency of the half-bridge inverter.

Therefore, since it is possible to control the output energy of the stage pulse magnetic stimulation device by simultaneously adjusting two output control parameters (the switching frequency and the pulse repetition rate), t was possible to vary the precise output of the magnetic stimulation device. The neuronal spike in activity can originate through the control signal wave structure in response to the new magnetic stimulation device, which may randomly form pulses through brain stimulation using FW-CW magnetic stimulation, consequently artificially creating an alpha wave state.

To increase accessibility, a GUI was developed using OLE automation objects to which component software based on object-oriented technology in the user interface was applied along with ADO technology. In addition, after measuring the vital signs separated from EEG and ECG spectra frequencies obtained from stimulating magnetic pulses with 90S8535 Chip (ATMEL Corporation), the brain activity was expressed succinctly in the GUI after image analysis and processing by data mining techniques using a PC and its interface.

Acknowledgement

This work was supported by the Dong-A University Research fund.

References

[1] J. F. Bates and P. S. Goldman-Rakic, Journal of Comparative Neurology **336**, 211 (1993).

[2] D. Bor, J. Duncan, A. C. H. Lee, A. Parr, and A. M. Owen, Neuropsychologia **44**, 229 (2006).

[3] S.-S. Choi, S.-M. Lee, and J.-H. Kim, J. Magnetics 213 (2010).

[4] S. Kosslyn, O. Koenig, A. Barrett, C. Cave, J. Tang, and J. D. E. Gabrieli, Journal of Experimental Psychology **15**, 723 (1989).

[5] H. B. Gak, J. Magnetics **16**, 51 (2011).

[6] S. Ueno, T. Tashiro, and K. Harada, J. Appl. Phys. **64**, 5862 (1988).

[7] L. G. Cohen, B. J. Roth, J. Nilsson, N. Dang, M. Panizza, S. Bandinelli, W. Friauf, and M. Hallett, Electroencephalogr. Clin. Neurophysiol. **75**, 350 (1990).

[8] V. E. Amassian, R. Q. Cracco, P. J. Maccabee, and J. B. Cracco, Electroencephalogr. Clin. Neurophysiol. **85**, 265 (1992).

[9] S.-S. Choi, Journal of Biomedicine and Biotechnology **2011**, 278062 (2011).

[10] L. A. Geddes and J. D. Bourland, in Magnetic Stimulation in Clinical Neurophysiology, S. Chokroverty, Ed. Butterworths, Boston (1990).

[11] M. Inghilleri, A. Berardelli, P. Marchetti, and M. Manfredi, Exp. Brain Res. **109**, 467 (1996).

[12] K. J. Werhahn, E. Kunesch, S. Noachtar, R. Benecke, and J. Classen, J. Physiol. **517**(Pt. 2), 591 (1999).

[13] A. Gadea and A. M. Lopez-Colome, J. Neurosci. Res. **64**, 218 (2001).

[14] M. Sandrini, A. V. Vergoni, and A. Bertolini, Pharmacol. Res. **28**, 47 (1993).